JOURNAL OF AGRICULTURAL AND FOOD CHEMISTRY

Isolation and Identification of Oligomers from Partial Degradation of Lime Fruit Cutin

SHIYING TIAN,[†] XIUHUA FANG,[†] WEIMIN WANG,[†] BINGWU YU,[†,‡] XIAOFANG CHENG,[†] FENG QIU,[§] ANDREW J. MORT,[§] AND RUTH E. STARK*[,†,‡]

Departments of Chemistry, College of Staten Island and City College of New York, City University of New York Graduate Center and Institute for Macromolecular Assemblies, New York, New York 10031, and Department of Biochemistry and Molecular Biology, Oklahoma State University, Stillwater, Oklahoma 74078

Complementary degradative treatments with low-temperature hydrofluoric acid and methanolic potassium hydroxide have been used to investigate the protective biopolymer cutin from *Citrus aurantifolia* (lime) fruits, augmenting prior enzymatic and chemical strategies to yield a more comprehensive view of its molecular architecture. Analysis of the resulting soluble oligomeric fragments with one- and two-dimensional NMR and MS methods identified a new dimer and three trimeric esters of primary alcohols based on 10,16-dihydroxyhexadecanoic acid and 10-oxo-16-hydroxyhexadecanoic acid units. Whereas only 10-oxo-16-hydroxyhexadecanoic acid units were found in the oligomers from hydrofluoric acid treatments, the dimer and trimer products isolated to date using diverse degradative methods included six of the seven possible stoichiometric ratios of monomer units. A novel glucoside-linked hydroxyfatty acid tetramer was also identified provisionally, suggesting that the cutin biopolymer can be bound covalently to the plant cell wall. Although the current findings suggest that the predominant molecular architecture of this protective polymer in lime fruits involves esters of primary and secondary alcohols based on long-chain hydroxyfatty acids, the possibility of additional cross-linking to enhance structural integrity is underscored by these and related findings of nonstandard cutin molecular architectures.

KEYWORDS: Fruit; *Citrus aurantifolia*; cuticle; cutin; oligomer; polyester; NMR; 2D NMR

INTRODUCTION

Plant cuticles in the leaves and fruit of terrestrial plants function primarily as protective barriers, controlling microbial attack as well as the diffusion of water and chemicals (*1*). These remarkable surfaces are capable of self-cleaning and can regulate their superlative mechanical performance during ripening. They consist of waxes and a structural support polymer, cutin. There are no known solvents for cutins, suggesting that they are heavily cross-linked polymers and/or bound to the plant cell wall. This intractability has hampered investigation of their covalent structure and domain architecture and thus has put limits on our understanding of their functions.

To meet this challenge and augment the well-established specifications of cutin monomeric constituents (*2*), the intact biopolymers from various fruits and leaves have been studied as dry or solvent-swelled solids using NMR spectroscopy (*3*−*9*) to identify chemical groupings and possible cross-link sites. In a complementary fashion, protocols that use enzymatic or chemical reagents to partially degrade the polymeric structure have been used to generate soluble oligomeric fragments that preserve the molecular architecture of the original cutin material. For instance, hydrolytic reagents have been used to generate homodimers and higher oligomers containing primary esters of dihydroxyhexadecanoic acid from tomato fruit cutin (*10, 11*), one of the most abundant monomers found in *Citrus* and tomato cutins (*12*). In addition, a tetramer consisting of two units of 10,16-dihydroxyhexadecanoic acid and two units of 10-oxo-16-hydroxyhexadecanoic acid was reported in lime fruit cutin (*13*). Finally, a pentamer consisting of four 10,16-dihydroxyhexadecanoic acid units and a less common monomer, linked entirely by secondary alcohol ester bonds, was reported from enzymatic degradation of limes (*14*).

In the present study, two complementary degradative procedures, using hydrofluoric acid (HF) and potassium hydroxide (KOH), respectively, have been used to generate soluble oligomers from lime fruit cutin. Preliminary structural characterization of these materials was described previously (*5*). Limes were chosen for these and prior studies because they offer an abundant source of cutin and have been reported to have a relatively simple monomer composition (*2, 15*). Low-temperature HF methods are known to cleave particular acetal bonds,

* To whom correspondence should be addressed. Tel: 212-650-8916. Fax: 212-650-8719. E-mail: stark@sci.ccny.cuny.edu.
[†] College of Staten Island.
[‡] City College of New York.
[§] Oklahoma State University.

10.1021/jf801028g CCC: $40.75
Published on Web 10/02/2008

removing sugars from glycoproteins but leaving the peptides intact (*16*) and breaking glycosidic acetal linkages of neutral sugars in polysaccharides in preference to amino or acidic sugars (*17*). Thus, the oligomeric fragments derived in this fashion from the cutin polyester may retain any hydroxyfatty acid linkages to sugars of the cell wall polysaccharides. To ensure that the resulting oligomers reflect the molecular structure of the polymer to a significant degree, a traditional methanolic KOH treatment, which breaks down accessible ester linkages readily, was also used. In the current work, the soluble oligomers were elucidated spectroscopically to gain insight into the chemical composition, covalent bonding patterns, and cross-link architecture of the cuticular polymer. These studies reveal that the monomers may be assembled in any possible order, that ester cross-links are rare or inaccessible to hydrolytic reagents, and that covalent connection of cutin to cell wall polysaccharides is also possible.

MATERIALS AND METHODS

Isolation of Lime Fruit Cutin. Cutin was isolated from the skin of lime fruits (*Citrus aurantifolia*) by a published three-step protocol (*18*): (i) peeling and subsequent separation of the cuticle by treatment with pectinase; (ii) enzymatic digestion of cell wall polysaccharides with successive cellulase, pectinase, and hemicellulase treatments; and (iii) exhaustive dewaxing by successive Soxhlet extraction with methanol, methylene chloride, and tetrahydrofuran. All reagents were obtained from Sigma (St. Louis, MO) or Aldrich (Milwaukee, WI) Chemical Cos. In a typical preparation, 200 limes yielded 5.0 g of dry cutin.

Lime Cutin Oligomers from HF. Anhydrous HF was reacted with 502 mg of powdered lime fruit cutin for 0.5 h at 0 °C and then quenched with diethyl ether in liquid nitrogen, cleaving saccharide bonds to produce oligomeric fragments (*19*). The ether−HF-soluble mixture (120 mg) was evaporated to dryness, and the resulting ethyl ester reaction products were extracted to yield chloroform- and water-soluble products (95 and 22 mg, respectively). The chloroform fraction was dried and then extracted with acetonitrile.

The acetonitrile extract was purified by reverse-phase high-performance liquid chromatography (HPLC) using Hewlett-Packard model 1100 equipment equipped with a quaternary solvent delivery system and both UV and diode array detectors (Agilent, Santa Clara, CA). Parallel observation of products lacking strong absorption at UV wavelengths was conducted using a Varex MKIII evaporative light scattering (ELSD) detector (Alltech, Deerfield, IL). Most separations were done using a 0.5 mL/min flow rate, gradient elution (acetonitrile/H_2O/THF, varied from 75:20:5 to 95:0:5 over 20 min), and 5 μm analytical and semipreparative C18 columns. ELSD detection used nitrogen gas pressurized at 26.6 psi and flowing at 2.19 L/min and a drift tube temperature of 65 °C. The isolated compounds (typically 0.5−0.7 mg from each of 10−18 fractions) were checked for purity by reinjection in two solvent systems using both UV and ELSD detection.

Lime Cutin Oligomers from KOH. To produce lime cutin oligomers with KOH, 500 mg of cutin was added to 100 mL of 1.5 M KOH solution in methanol. The mixture was stirred at room temperature overnight. Then, the reacted mixture was acidified to pH 5 with 10% HCl and filtered. The unreacted residue was washed with water to remove the salt, then dried in air prior to examination by magic-angle spinning NMR. The filtrate was also dried in air, and the products were then extracted with 30 mL of 1:1 v/v chloroform/methanol five times until only white salt remained. The extracts were combined and dried under vacuum.

The extracted products were subjected to silica gel column chromatography and eluted using a hexane/acetone system with step gradients. Twenty fractions were collected, and each fraction was purified further using high-performance thin-layer chromatography (HPTLC) with a hexane/acetone elution system. Isolated compounds (typical yield, 0.5 mg) were checked for purity as described above.

NMR Spectroscopy. A Varian UNITY INOVA spectrometer operating at a ^{1}H frequency of 599.95 MHz, outfitted with an inverse-detection HX nanoprobe and pulsed field gradients, was used to collect NMR spectra of the cutin oligomers. Each 40 μL sample was dissolved in $CDCl_3$ containing 1% tetramethylsilane (TMS) (Aldrich) to provide a field-frequency lock and an internal chemical shift reference. Typical experimental conditions for one-dimensional (1D) ^{1}H experiments included 16 repetitions separated by 2.0 s delays and a spectral width of 7200 Hz defined by 26240 time-domain points. VNMR software was used to process the data and integrate the ^{1}H peak areas. Database software from Advanced Chemistry Development (Toronto, Canada) was used to make ^{13}C and ^{1}H chemical shift predictions.

To establish through-bond connections within and between monomer units of the oligomer structures, both homo- and heteronuclear two-dimensional (2D) NMR data were acquired. ^{1}H−^{1}H total correlation spectroscopy ("clean" TOCSY) (*20*) experiments were conducted with a mixing period of 70 ms and spin-lock field of 6.25 kHz to permit polarization transfer throughout each scalar-coupled spin system. ^{1}H-detected heteronuclear multiple quantum coherence (^{13}C HMQC) spectroscopy (*21*) with a magnetization transfer time corresponding to $^1J_{CH} = 140$ Hz was used to identify bonded proton−carbon pairs. ^{13}C decoupling was done with the GARP sequence (*22*); coherence selection and suppression of spectral artifacts were achieved using pulsed field gradients (*23, 24*). Spectral widths of 7200 Hz for ^{1}H and 27150 Hz for ^{13}C were typically used for HMQC experiments, which included a relaxation delay of 1.0 s between transients and a 2D matrix of 2K × 256 points, zero-filled to 2K × 1K points to enhance spectral resolution. Heteronuclear multiple-bond correlation (^{13}C HMBC) spectroscopy (*25*) with a polarization transfer time corresponding to $^3J_{CH} = 10$ Hz was employed to delineate long-range proton−carbon interactions.

Mass Spectrometry. Mass spectral data were acquired on three instruments: Agilent Technologies 1100 Series LC/MSD model G1946D, model SL, and TOF-MS model 6210 (Santa Clara, CA). Electrospray ionization (ESI) was carried out with a drying gas temperature of 175 °C, a nebulizer pressure of 40 psi, and a flow rate of 13 L/min. Masses were scanned between 200 and 1500 *m/z*, using fragmenter values between 60 and 250 V depending on whether molecular ions or fragments were desired. The capillary voltage was set to 3500 V. Samples were introduced into the mass spectrometer in a 1:1 mixture of water and acetonitrile containing 0.1% acetic acid and 50 μM ammonium acetate. ESI-MS^n was conducted with ionization agents including 0.1% formic acid and 10 mM ammonium formate in a methanol−water solvent, whereas TOF-MS was done using 0.1% acetic acid in methanol−water. Data were processed using Agilent Chemstation software.

RESULTS AND DISCUSSION

Oligomers from HF-Treated Lime Cutin. As reported previously (*5*), the typical yield of soluble products from this treatment was 23%, a significant improvement over published enzymatic methods (*14*). The oligomeric compounds from HF-treated lime cutin were isolated in the current study as ethyl esters of carboxylic acids (presumably from workup with diethyl ether) and had free alcohol groups at the other terminus, suggesting that some ester linkages, as well as the expected acetals, may be cleaved. Compound **1** (**Figure 1**) was elucidated as a dimer containing two units of 10-oxo-16-hydroxy-hexadecanoic acid with a primary ester linkage. With the identification of this dimer, each of the three possible primary ester stoichiometries of the two predominant *Citrus* cutin monomers (10-oxo-16-hydroxyhexadecanoic acid and 10,16-dihydroxy-hexadecanoic acid) has been found among the degradation products of lime fruit cutin (*9, 12*).

The ESI-MS spectrum exhibited three types of molecular ions: *m/z* 583 [M + H^+], 600 [M + NH_4^+], and 605 [M + Na^+], corresponding to a molecular formula of $C_{34}H_{62}O_7$. In the absence of fragment ions, the positions of the oxo groups were assumed from structures of the known monomers (*12*).

The proposed molecular structure of **1** was supported by its NMR spectra (**Table 1**). Integrated intensities in the 1D 600 MHz ^{1}H NMR spectrum were reasonably consistent with the

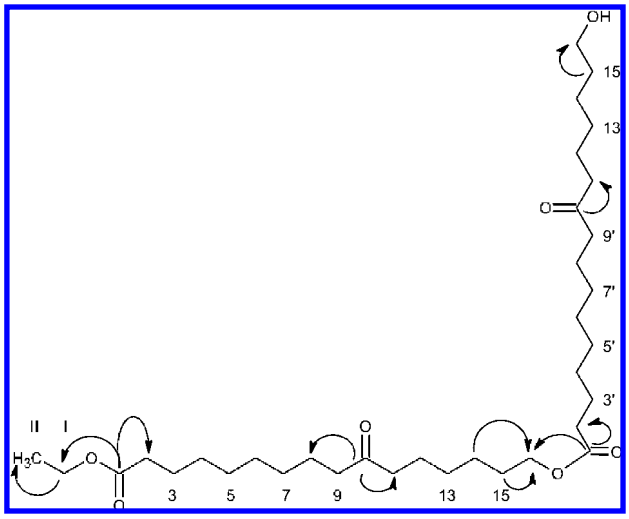

Figure 1. Significant HMBC (C→H) correlations for compound **1**.

Table 1. NMR Spectral Data for Compound **1** ($CDCl_3$) from HF Treatment

position	functional group[a]	δ_H (ppm)[b]	δ_C (ppm)[b]
1, 1′	COO		173.9
2, 2′	**CH_2**COO	2.26 (t, 5H)	34.2
3−7, 3′−7′, 13, 13′, 14, 14′	(**CH_2**)$_n$, **$CH_2CH_2CH_2$**C=O, **$CH_2CH_2CH_2$**OC	1.24 (m)[c]	29.1
8, 8′, 12, 12′	**CH_2CH_2**C=O	1.54 (b)	24.1
9, 9′, 11, 11′	**CH_2**C(O)**CH_2**	2.36 (t, 8H)	42.5
10, 10′	C=O		211.0
15	**CH_2CH_2**OC=O	1.58 (b)	24.3
15′	**CH_2CH_2**OH	1.60 (b)	28.0
16	**CH_2**OC(O)	4.05 (t, 3H)	63.8
16′	**CH_2**OH	3.62 (t, 3H)	62.9
I	CH_3**CH_2**OC(O)	4.11 (q, 2H)	60.1
II	**CH_3**CH_2OC(O)	1.22 (t, 3H)[c]	14.2

[a] Nuclei for which HMQC correlations were observed are shown in bold. [b] Referenced to internal tetramethylsilane. Integrals and multiplicities from the 1D ^{1}H spectrum are indicated in parentheses. [c] Overlapping peaks and large relative size make integration unreliable.

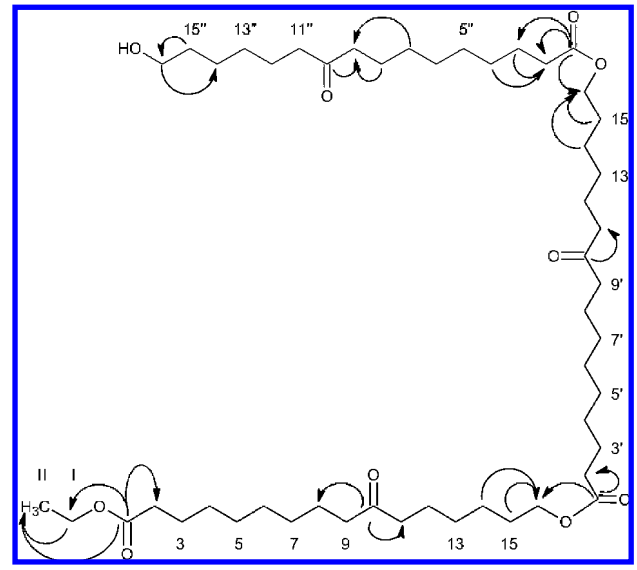

Figure 2. Significant HMBC (C→H) correlations for compound **2**.

Table 2. NMR Spectral Data for Compound **2** ($CDCl_3$) from HF Treatment

position	functional group[a]	δ_H (ppm)[b]	δ_C (ppm)[b]
1, 1′, 1″	COO		173.9
2, 2′, 2″	**CH_2**COO	2.26, t, 6H	33.7
3−8, 3′−8′, 3″−8″, 12−15, 12′−15′, 12″−15″	(**CH_2**)$_n$, **CH_2CH_2**C=O, **CH_2CH_2**OC=O, **CH_2CH_2**OH	0.8−2.0 (m)[c]	24.0, 28.9
9, 9′, 9″, 11, 11′, 11″	**CH_2**C(O)**CH_2**	2.36, (t, 10H)	42.5
10, 10′, 10″	C=O		211.0
16″	**CH_2**OH	3.62, t, 2H	62.9
16, 16′	**CH_2**OC(O)	4.05, t, 4H	63.8
I	CH_3**CH_2**OC(O)	4.11, q, 2H	60.1
II	**CH_3**CH_2OC(O)	1.22 (t, 3H)	14.2

[a] Nuclei for which HMQC correlations were observed are shown in bold. [b] Referenced to internal tetramethylsilane. Integrals and multiplicities from the 1D ^{1}H spectrum are indicated in parentheses. [c] Overlapping peaks and large relative size make integration unreliable.

proposed structure: In addition to large $(CH_2)_n$ signals, key resonances were observed for H-2,2′ (2.26 ppm, t, 5H), H-9,9′ and H-11,11′ (2.36 ppm, t, 8H), H-16′ (3.62 ppm, t, 3H), H-16 (4.05 ppm, t, 3H), and H-I (4.11 ppm, q, 2H). The gradient-assisted heteronuclear multiple quantum correlation (gHMQC) 2D NMR spectrum identified directly bonded protons and carbons, showing diagnostic correlations for particular molecular moieties: −**CH_2**COO− (2.26, 34.2 ppm), −**CH_2**C(O)**CH_2**− (2.36, 42.5 ppm), HO**CH_2**− (3.62, 62.9 ppm), −**CH_2**OC(O)− (4.05, 63.8 ppm), and CH_3**CH_2**OC(O)− (4.11, 60.1 ppm). Numerous correlations were also observed for the bulk methylene groups. ^{1}H−^{1}H TOCSY spectra supported through-bond connectivities of the $(CH_2)_n$ groups with CH_2s that were shifted downfield by oxygen (data not shown). Finally, gradient-assisted HMBC spectroscopy (gHMBC) (**Figure 1**) gave information on ^{1}H−^{13}C pairs separated by two or three bonds. Cross-peaks between ^{13}C at 173.9 ppm and ^{1}H nuclei at both 4.04 and 4.11 ppm were diagnostic for esters of primary alcohols (*13*), strongly supporting the proposed structure.

Compound **2** (**Figure 2**) was identified as a trimer consisting of three 16-hydroxyl-10-oxo-hexadecanoic acid units. ESI-MS exhibited two types of molecular ions: *m*/*z* 868 [M + NH_4^+] and 873 [M + Na^+], corresponding to a molecular formula of $C_{50}H_{90}O_{10}$. No fragments of these ions were available to confirm the positions of the oxo groups assumed from earlier monomer elucidations (*12*), but the observation of isotopic peaks with 50% of the parent peak intensity was in agreement with the proposed trimer structure containing 50 carbons.

The molecular structure of **2** was supported by its NMR spectra (**Table 2**). As anticipated from the similarity of their monomeric building blocks, the 1D and 2D NMR spectra of **2** were similar to those of **1**. Key gHMBC correlations, including those that were diagnostic for esters of primary alcohols (*13*), are summarized in **Figure 2**.

Several additional compounds were isolated by HPLC methods. One- and two-dimensional NMR as described above indicated two dimers composed of one unit each of 10,16-dihydroxyhexadecanoic acid and 10-oxo-16-hydroxyhexadecanoic acid but distinguished by their elution times. Although their molecular structures could not be confirmed by MS methods, provisional identifications could be made from the NMR data because both the monomeric constituents and the dimer structures are known (*1, 13*). Another compound, provisionally identified as **3** (**Figure 3**), had both NMR features resembling the oligomers described above and additional characteristic spectroscopic signatures for sugar rings and double bonds (**Table 3**).

The ^{1}H NMR integrals, coupled with ^{1}H−^{13}C HMQC- and HMBC-derived connectivity information, indicated the following structural units that were essentially identical to **1** and **2**: four −**CH_2**COO− groups (2.26, 34.7 ppm; HMBC at 174.0 ppm), three −**CH_2**OC(O)− groups (4.04, 64.2 ppm and 4.09,

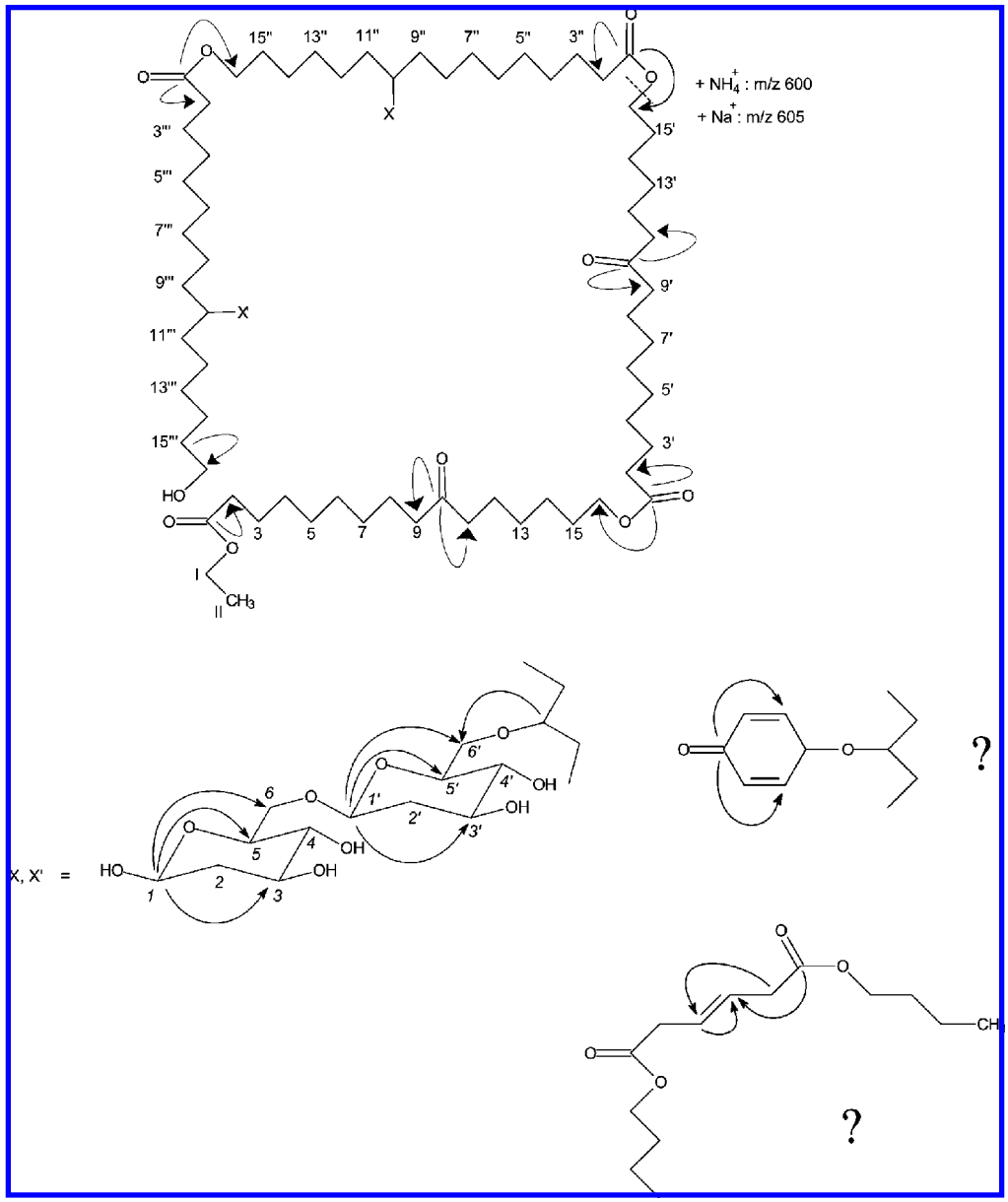

Figure 3. Significant HMBC (C→H) correlations for provisionally identified compound **3**. Fragments corresponding to sodium and ammonium adducts from the designated cleavage were observed in the mass spectrum (see text). The positions of the midchain substituents are designated by analogy with the predominant reported fruit cutin monomers (*15*).

60.4 ppm; HMBC to 174 ppm), two −**CH**$_2$C(O)**CH**$_2$− groups (2.36, 42.8 ppm; HMBC to 211 ppm), two HO**CH**$_2$− groups (3.62, 62.7 ppm; HMBC to 32.6 ppm), one CH$_3$**CH**$_2$OC(O)− group (4.11, 60.2 ppm), and one **CH**$_3$CH$_2$OC(O)− group (1.24, 14.0 ppm). Thus, in analogy to **1** and **2** from the same HF treatment, compound **3** was deduced to be an ethyl ester-terminated tetramer based on 10-oxo-16-hydroxyhexadecanoic acid units linked by esters of primary alcohols. As noted in **Figure 3** and described for compound **1**, ESI-MS of **3** yielded strong peaks at *m*/*z* 600 and 605, in this case corresponding to the ammonium and sodium adducts of two sequential midchain oxo monomeric units, that is, cleavage of the proposed structure at a weak C−O bond. No ions corresponding to higher molecular weights were observed in the mass spectrum, but the MS provided confirmatory evidence for the dimer portion comprised of two *ω*-hydroxy-10-oxo-hexadecanoic acid monomer units.

To devise a structural hypothesis consistent with the remaining NMR data, we considered the known *Citrus* cutin monomers, glycerol and dicarboxylic acids, found recently in other cutins (*26, 27*) and plant oxylipins involved in plant defense (*28*), which have also been reported covalently linked to sugars (*29*). Although none of these possibilities was entirely consistent with the NMR data, several structural conclusions could be drawn from the data: (i) Compound **3** contains two additional primary ester linkages, verified by ^{1}H resonances at 2.26 ppm (4H) that are linked in HMBC spectra to carboxyl carbons at 174 ppm; (ii) the third and fourth hydroxyfatty acid "legs" of the structure do not bear midchain oxo, hydroxyl, or aliphatic ester functionalities, for which diagnostic α-proton resonances would be expected at 2.36 ppm or methine proton signals at 3.56 and 4.84 ppm, respectively; (iii) the −**CH**$_2$COO− carbons observed at 34.7 ppm are linked by HMBC to multiply bonded groups at 6.54 and 6.59 ppm; and (iv) the protons at 6.54 and 6.59 ppm, which are directly bound to carbons at 140.7 and 141.5 ppm, also have long-range covalent links to a carbon at 186.7 ppm. Although no known cutin monomers account for the spectral features described in iii and iv, for the sake of

Table 3. NMR Spectral Data for Compound **3** ($CDCl_3$) from HF Treatment

position	functional group[a]	δ_H (ppm)[b]	δ_C (ppm)[b]
1, 1′, 1″	COO		174.0
2, 2′, 2″; 2‴	**CH_2**COO	2.26 (t, 8H)	34.6; 34.7, 34.8
3−7, 3′−7′, 3″−7″, 3‴−7‴, 13′, 13″, 13″; 13‴, 14, 14′, 14″, 14‴	(**CH_2**)$_n$	1.2 (m)[c]	29.1
8, 8′, 8″, 8‴, 12, 12′, 12″, 12‴, 15, 15′, 15″, 15‴	**CH_2CH_2**C=O, **CH_2CH_2**OC=O	∼1.6 (m)[c]	25.1
9, 9′, 11, 11′	**CH_2**C(O)**CH_2**	2.36 (t, 8H)	42.8
10, 10′	CH_2**C(O)**CH_2		211.3
16, 16′; 16″	**CH_2**OC(O)	4.04 (t, 4H); 4.09 (m, 2H)	64.2, 60.4
16‴	**CH_2**OH	3.62 (m, 2H)	62.7
I	CH_3**CH_2**OC(O)	4.11 (m or q, 2H)	60.2
II	**CH_3**CH_2OC(O)	1.24 (m)[c]	14.0
10″, 10‴	CHO-X	4.20 (m, 2H)	72.7
X, X′	**CH=CH**	6.54, 6.59 (d,d, 4H, J = 2.7)	140.7, 141.5
X, X′	HC=CH**C(O)**CH=CH		186.7
1, 1′	sugar H-1, H-1′	5.62, 5.51 (d, d, 1H, 1H, J = 2.7)	106.2, 107.5
2, 2′	deoxy sugar H-2, H-2′	1.60,[c] 1.84	25.1
3, 3′	sugar H-3, H-3′	3.84 or 3.93 (m, 2H ea)	67.3
4, 4′	sugar H-4, H-4′	3.89 (m, 2H)	67.3
5, 5′	sugar H-5, H-5′	3.84, 3.85, or 3.93 (m, 2H)	67.3
6, 6′	disaccharide H-6, aglycon H-6′	3.64, 3.75 (m, 4H)	63.1, 60.4

[a] Nuclei for which HMQC correlations were observed are shown in bold. [b] Referenced to internal tetramethylsilane. Integrals and multiplicities from the 1D ^{1}H spectrum are indicated in parentheses. [c] Overlapping peaks and large relative size of the $(CH_2)_n$ signals make integrations unreliable. The methyl group is buried under the bulk methylenes in the 1D ^{1}H spectrum but clearly distinguished in 2D HMQC.

concreteness, **Figure 3** displays two symmetric doubly bonded fragments that could be attached at a midchain location or to a carbonyl group.

In addition, compound **3** exhibited NMR signals with diagnostic chemical shifts and coupling patterns for a disaccharide, although its solubility in chloroform and acetonitrile suggests a glycoside linked to the hydroxyfatty acid oligomer. The provisional disaccharide structure and corresponding HMBC correlations appear in **Figure 3**. Thus, although incomplete spectral data prevent definitive verification of the structure of **3**, many architectural features including a plausible linkage to the cell wall are evident. Using ACD chemical shift simulations and observed 2D NMR through-bond connectivities as a guide, our hypothesis includes an ether linkage and deoxy hexose sugars joined by a β1→6 linkage. A key element of the proposal is a methine resonance at (4.20, 72.7 ppm), which is linked by HMBC to the aglycone protons at 3.75 ppm and not coupled to the sugar ring resonances. A β1→4 linkage, such as might be expected from cellulose in the cell wall, was also consistent with the observed 2D NMR correlations but in worse agreement with the ACD simulations. Mild degradation protocols are under development in our laboratory to permit fuller characterization of these interesting structural moieties.

Separation and Identification of Oligomers from KOH-Treated Lime Cutin. A 60% yield of soluble products was achieved from this degradative treatment, far exceeding the 5% obtained with porcine pancreatic lipase and 23% obtained with low-temperature HF reagents, respectively. As expected from prior monomer analyses (*15, 30*), the predominant products were midchain substituted (oxo and hydroxy) hydroxyfatty acids (data not shown). The oligomers from KOH treatment of lime fruit cutin were isolated as methyl esters of carboxylic acids, with free alcohols at the other terminus.

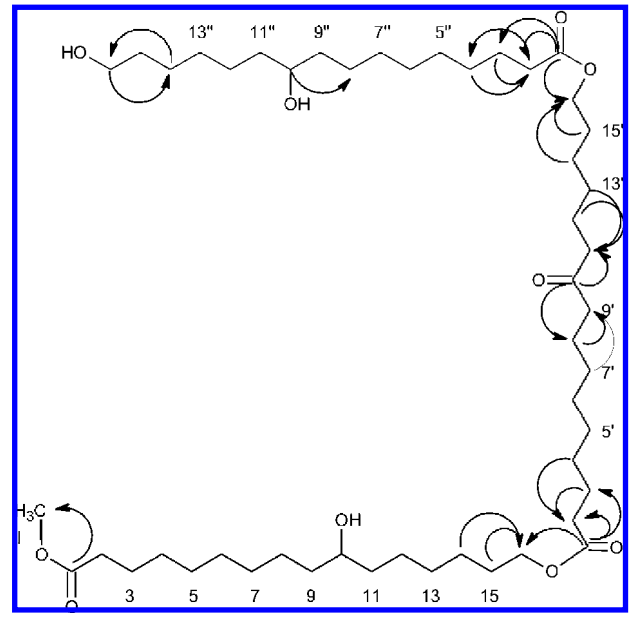

Figure 4. Significant HMBC (C→H) correlations for compound **4**.

Table 4. NMR Spectral Data for Compound **4** ($CDCl_3$) from KOH Treatment

position	functional group[a]	δ_H (ppm)[b]	δ_C (ppm)[b]
1, 1′, 1″	COO		173.9
2, 2′, 2″	**CH_2**COO	2.26 (t, 8H)	34.4
3−7, 3′−7′, 3″−7″, 13, 14, 13′, 14′, 13″, 14″	(**CH_2**)$_n$	1.24 (m)[c]	29.1
8, 8′, 8″, 12, 12′, 12″; 9, 9″, 11, 11″	**CH_2CH_2**C=O; **CH_2**CHOH	1.54 (m)[c]	25.1
9′, 11′	**CH_2**C(O)**CH_2**	2.36 (t, 5H)	42.6
10′	C=O		211.0
10, 10″	**CH**OH	3.56 (m,2H)	71.9
15, 15′	**CH_2CH_2**OC=O	1.58	24.3
15″	**CH_2CH_2**OH	1.60	28.0
16″	**CH_2**OH	3.62 (t, 2H)	62.5
16, 16′	**CH_2**OC(O)	4.04 (t, 4H)	63.8
I	**CH_3**OC(O)	3.64 (s, 3H)	51.1

[a] Nuclei for which HMQC correlations were observed are shown in bold. [b] Referenced to internal tetramethylsilane. Integrals and multiplicities from the 1D ^{1}H spectrum are indicated in parentheses. [c] Overlapping peaks and large relative size make integration unreliable.

Compound **4** (**Figure 4**) was determined as a trimer comprised of two units of 10,16-dihydroxyhexadecanoic acid and one unit of 10-oxo-16-hydroxyhexadecanoic acid. As compared with **1**−**3**, this compound exhibited unique ^{1}H NMR resonances attributable to secondary alcohol protons (10 and 10″, 3.56 ppm, m) and the methyl group of a terminal ester (I, 3.64 ppm, s). The secondary alcohol moiety was confirmed by a gHMQC cross-peak for a directly bonded H−C pair at (3.56, 71.9 ppm) and a gHMBC cross-peak between that carbon and the adjacent methylene protons at (1.54, 71.9 ppm). No HMBC cross-peaks were observed to the proton of the secondary alcohol group, presumably because the resonance is weak and split into a multiplet. Support for the proposed structure of **4** also came from HMQC correlations summarized in **Table 4**, and linkages of the monomers through esters of primary alcohols (*13*) were supported by a key HMBC cross-peak at (4.04, 173.9 ppm) (**Figure 4**).

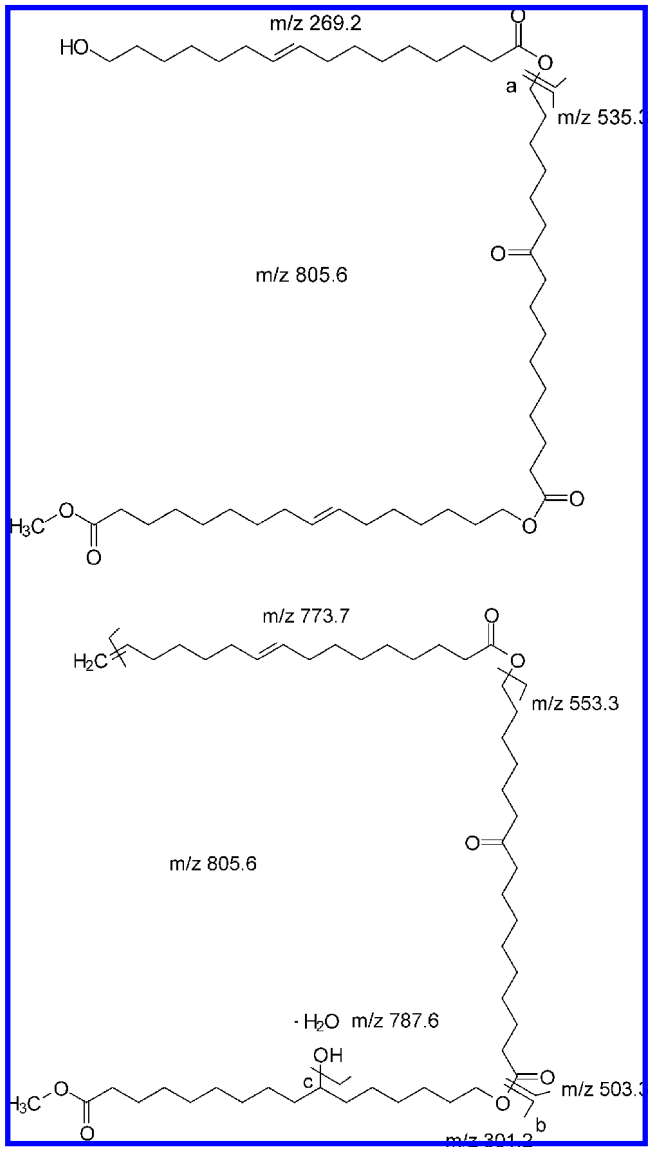

Figure 5. Proposed MS fragmentation patterns for compound **4**.

The ESI-MS spectrum of **4** exhibited three types of molecular ions: *m/z*841.7 [M + H^+], 858.7 [M + NH_4^+], and 863.7 [M + Na^+], corresponding to a molecular formula of $C_{49}H_{92}O_{10}$. The isotopic peaks (molecular ions + 1) were about 55% as intense as the original peaks, consistent with a trimer structure containing 49 carbons. TOF-MS gave [M + H^+] and [M + Na^+] ions at 841.6765 and 863.6572, respectively, confirming the $C_{49}H_{92}O_{10}$ molecular formula.

ESI-MS^n experiments were also conducted to establish the order of monomer units within the released cutin trimer. MS^2 of the ion at *m/z* 841.7 corresponding to [M + H^+] yielded major peaks in the spectrum at 823.6, 805.6, and 787.6 from the elimination of three successive H_2O molecules. MS^3 of the most intense 805.6 peak produced ions at *m/z* 787.6, 773.6, **553.3**, 535.3, **301.2**, 283.3, and 269.2, where the ions in bold were also observed in MS^2. As shown in **Figure 5**, the MS^3 fragments correspond to breakage at "a" to yield 535.3 + 269.2, breakage at "b" to yield 503.3 + 301.2, or breakage at "b" and "c" to yield 503.3 + 283.3, depending on which ester bond breaks and whether a molecule of water has also been lost. Both the 535.3 and the 503.3 fragments implicate adjacent monomer units with midchain oxo and hydroxyl functionalities but are not consistent with sequential 10-hydroxyhexadecanoic acid units. Additionally, the absence of a fragment at 299 rules out a midchain oxo monomer at the methyl ester terminus of the trimer. Finally, MS^4 of the strong peak at *m/z* 553.5 gave strong ions at 535.7, 521.6, and 301.2, corresponding to the elimination of H_2O, a terminal CH_3OH group, and oxo-acylium group, respectively. Together, these fragmentation data establish a pattern of alternating midchain OH, oxo, and OH groups in the lime cutin trimer **4**.

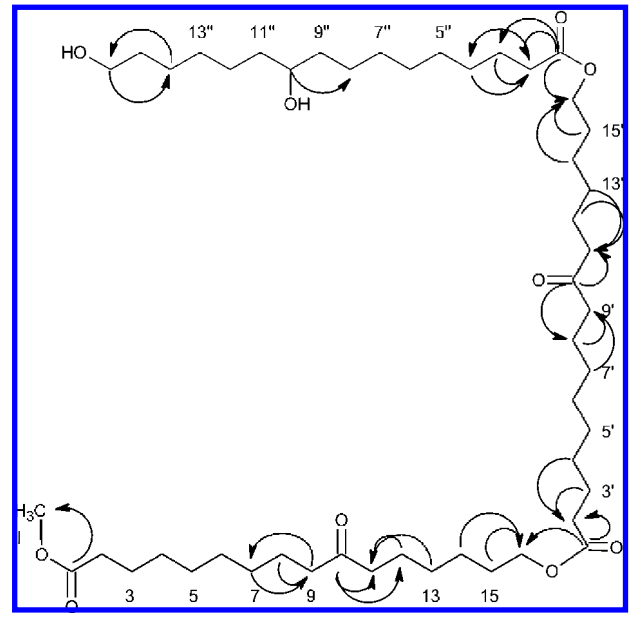

Figure 6. Significant HMBC (C→H) correlations for compound **5**. (The order of the acyl-containing monomeric units is undetermined.)

Compound **5** (**Figure 6**) was identified as a trimer consisting of one unit of 10,16-dihydroxyhexadecanoic acid and two units of 10-oxo-16-hydroxyhexadecanoic acid. Its ESI-MS spectrum exhibited two types of molecular ions, *m/z* 856 [M + NH_4^+] and 861 [M + Na^+], corresponding to a molecular formula of $C_{49}H_{90}O_{10}$. No M + H^+ molecular ion or fragments were found, but isotopic peaks with intensities about 55% as large as the original peaks were consistent with a trimer structure containing 49 carbons. In the absence of fragments from cleavage of the midchain functional groups, the positions of the midchain oxo and hydroxyl groups were assumed from the structures of the known monomers (*12*) as before, and the sequence of monomer units within the trimer remained undetermined.

The molecular structure of **5** was deduced from its NMR spectra (**Table 5**). The 1D and 2D NMR data of compound **5** were similar to those collected for **4**, with the most significant differences involving integrals of the respective ^1H spectra. As described above for compound **4**, diagnostic peaks were observed in the ^1H NMR spectrum for secondary alcohol and methyl ester groups at 3.56 and 3.64 ppm, respectively. Cross-peaks at (3.56, 71.9 ppm) in gHMQC and at (1.54, 71.9 ppm) in gHMBC served to confirm the presence of a secondary alcohol group in **5**, analogous to the spectral features exhibited by **4**. An HMBC correlation at (4.04, 173.9 ppm) implicated the proposed monomer linkages through esters of primary alcohols (*13*) (**Figure 6**).

DISCUSSION

The studies presented herein provide a more comprehensive picture of the molecular architectures present in lime fruit cutin, augmenting prior compositional information derived from spectroscopic examination of the monomeric constituents, the intact solid biopolymer, and selected oligomers.

Table 5. NMR Spectral Data for Compound **5** ($CDCl_3$) from KOH Treatment

position	functional group[a]	δ_H (ppm)[b]	δ_C (ppm)[b]
1, 1′, 1″	COO		173.9
2, 2′, 2″	**CH_2**COO	2.26 (t, 7H)	34.4
3−7, 3′−7′, 3″−7″, 13, 14, 13′, 14′, 13″, 14″	**$(CH_2)_n$**	1.24 (m)[c]	29.1
8, 8′, 8″, 12, 12′, 12″; 9″, 11″	**CH_2CH_2C**=O; **CH_2**CHOH	1.54	25.1
9, 9′, 11, 11′	**$CH_2C(O)CH_2$**	2.36 (t, 6H)	42.6
10, 10′	C=O		211.0
10″	**CH**OH	3.56 (m, 1H)	71.9
15, 15′	**CH_2CH_2**OC=O	1.58	24.3
15″	**CH_2CH_2**OH	1.60	28.0
16″	**CH_2**OH	3.62 (t, 2H)	62.5
16, 16′	**CH_2**OC(O)	4.04 (t, 4H)	63.8
I	**CH_3**OC(O)	3.64 (s, 3H)	51.1

[a] Nuclei for which HMQC correlations were observed are shown in bold. [b] Referenced to internal tetramethylsilane. Integrals and multiplicities from the 1D ^1H spectrum are indicated in parentheses. [c] Overlapping peaks and large relative size make integration unreliable.

Although the modest yields of isolated products argue for caution in interpretation, a number of conclusions may be drawn regarding the biopolymer structure. As expected, the constituents of most of the oligomers reported herein are 10-oxo-16-hydroxyhexadecanoic acid (A) and 10,16-dihydroxyhexadecanoic acid (B), the most abundant monomers derived from alkaline or acidic depolymerization. Taking into account both current and prior studies of this fruit cutin, each of the possible pairs of abundant monomers (AA, AB, BB) is represented among the dimer products; similarly, three different monomer compositions are represented among the isolated trimers (AAA, AAB, ABB). These compositions are reasonable, given that similar proportions of A and B account for nearly 99% of the isolated monomers (*12*). Nonetheless, the HF treatment yielded **1** and **2** comprised of only 10-oxo-16-hydroxyhexadecanoic acid units (A), perhaps because products rich in B units are prone to further breakdown. By contrast, the oligomers from KOH included a trimer with an alternating BAB sequence, suggesting that both major monomers could be available simultaneously for incorporation into the polymer during cutin biosynthesis. Such mixed-monomer architectures also offer the possibility of strengthening the cutin polymeric network by hydrogen bonding between midchain oxo and hydroxyl groups.

Although we have reported esters of secondary alcohols from degradation of lime fruit cutin by porcine pancreatic lipase (*14*) or controlled alkaline hydrolysis (*31*), only dimer and trimer esters of primary alcohols were isolated from the soluble products of the current low-temperature HF and methanolic KOH treatments. These treatments leave most of the secondary ester moieties intact, hypothetically because they are located in densely cross-linked regions that are inaccessible to soluble degradative reagents and/or simply more sterically hindered than the corresponding primary ester linkages.

Our proposal of a hydroxyfatty acid tetramer linked to the C_6 position of a hexose-based disaccharide adds to the growing list of novel or minor plant cutin constituents, with as-yet-undetermined structural and functional significance. For instance, trace amounts of coumaric acid and from 1 to 15% glycerol monomers have been reported among the soluble monomers from base hydrolysis of *Lycopersicon esculentum* fruits and *Citrus aurantium* leaves (*26*), whereas >50% unsaturated dicarboxylic acids have been reported from *Arabidopsis thaliana* stem epidermis (*27*). Among the oligomers from mild degradative treatments that can reveal essential cuticular biopolymer architecture, we have found a pentamer including an atypical 1,7,16-trihydroxyhexadecanol unit and linked entirely by esters of secondary alcohols (*14*) as well as a trimer with midchain esterification through a secondary alcohol (*9*) from lime fruit cutin; Graça and co-workers have isolated monoacylglyceryl esters from several leaf cutins (*26*). Finally, cutin architectures involving α-branched fatty acids/esters have been reported for intact cuticles of *L. esculentum* fruit and *Agave americana* leaves (*7, 8*), although the use of strongly oxidizing oxalate and *para*-periodate solutions in sample preparation argues for caution in the interpretation of these findings. Although the predominant molecular architecture of the cutin biopolymer in lime fruits evidenced to date involves esters of primary and secondary alcohols based on long-chain hydroxyfatty acids, it has been pointed out that such linkages result in dendrimer architectures (*27*) rather than a cross-linked architecture. Thus, a variety of "nonstandard" bonding patterns, whether through ethers or to cell wall polysaccharides, may also serve as molecular bridges that can bolster the structural integrity of the plant cuticular netting and modulate its resilient interactions with both the cell wall and the wax constituents at its interface to the external environment.

ACKNOWLEDGMENT

The NMR Facility is operated by the College of Staten Island (CSI) and the CUNY Institute for Macromolecular Assemblies, a Center of Excellence of the Generating Employment through New York State Science program. We acknowledge the generous assistance of Dr. Hsin Wang in optimizing the 2D NMR experiments. Dr. Cliff Soll ran some of the MS experiments and helped to analyze the MS data. The CSI HPLC/MS Facility (Agilent SL) is operated by The College of Staten Island and the CUNY Institute for Macromolecular Assemblies. Farah Jayman assisted with the isolation of lime cutin; Drs. Tony Bin Yan and Daniel Arrieta-Baez provided critical input on the structural elucidations.

LITERATURE CITED

(1) Kolattukudy, P. E. Biochemistry and function of cutin and suberin. *Can. J. Bot.* **1984**, *62*, 2918–2933.
(2) Pollard, M.; Beisson, F.; Li, Y.; Ohlrogge, J. Building lipid barriers: Biosynthesis of cutin and suberin. *Trends Plant Sci.* **2008**, *13*, 236–246.
(3) Zlotnik-Mazori, T.; Stark, R. E. Nuclear magnetic resonance studies of cutin, an insoluble plant polyester. *Macromolecules* **1988**, *21*, 2412–2417.
(4) Stark, R. E.; Yan, B.; Ray, A. K.; Chen, Z.; Fang, X.; Garbow, J. R. NMR studies of structure and dynamics in fruit cuticle polyesters. *Solid State NMR* **2000**, *16*, 37–45.
(5) Fang, X.; Qiu, F.; Yan, B.; Wang, H.; Mort, A. J.; Stark, R. E. NMR studies of molecular structure in fruit cuticle polyesters. *Phytochemistry* **2001**, *57*, 1035–1042.
(6) Round, A. N.; Yan, B.; Dang, S.; Estephan, R.; Stark, R. E.; Batteas, J. D. The influence of water on the nanomechanical behavior of the plant biopolyester cutin as studied by AFM and solid-state NMR. *Biophys. J.* **2000**, *79*, 2761–2767.
(7) Deshmukh, A. P.; Simpson, A. J.; Hatcher, P. G. Evidence for cross-linking in tomato cutin using HR-MAS NMR spectroscopy. *Phytochemistry* **2003**, *64*, 1163–1170.

(8) Deshmukh, A. P.; Simpson, A. J.; Hadad, C. M.; Hatcher, P. G. Insights into the structure of cutin and cutan from *Agave americana* leaf cuticle using HRMAS NMR spectroscopy. *Org. Geochem.* **2005**, *36*, 1072–1085.

(9) Stark, R. E.; Tian, S. The cutin biopolymer matrix. In *Biology of the Plant Cuticle*; Riederer, M., Müller, C., Eds.; Blackwell Publishing Co.: Oxford, United Kingdom, 2006.

(10) Osman, S. F.; Gerard, H. C.; Fett, W. F.; Moreau, R. A.; Dudley, R. L. Method for the production and characterization of tomato cutin oligomers. *J. Agric. Food Chem.* **1995**, *43*, 2134–2137.

(11) Osman, S. F.; Irwin, P. L.; Fett, W. F.; O'Connor, J. V.; Parris, N. Preparation, isolation, and characterization of cutin monomers and oligomers from tomato peels. *J. Agric. Food Chem.* **1999**, *47*, 799–802.

(12) Deas, A. H. B.; Holloway, P. J. The intermolecular structure of some plant cutins. In *Lipids and Lipid Polymers in Higher Plants*; Tevini, M., Lichenthaler, H. K., Eds.; Springer-Verlag: Berlin, 1977; pp 293−299.

(13) Ray, A. K.; Chen, Z.; Stark, R. E. Chemical depolymerization studies of the molecular architecture of lime fruit cuticle. *Phytochemistry* **1998**, *49*, 65–70.

(14) Ray, A. K.; Stark, R. E. Isolation and molecular structure of an oligomer produced enzymatically from the cuticle of lime fruit. *Phytochemistry* **1998**, *48*, 1313–1320.

(15) Holloway, P. J. The chemical constitution of plant cutins. In *The Plant Cuticle*; Cutler, D. F., Alvin, K. L., Price, C. E., Eds.; Academic Press: New York, 1982.

(16) Mort, A. J.; Lamport, T. A. Anhydrous hydrogen fluoride deglycosylates glycoproteins. *Anal. Biochem.* **1977**, *82*, 289–309.

(17) Mort, A. J.; Bauer, W. D. Application of two new methods for cleavage of polysaccharides into specific oligosaccharide fragments. Structure of the capsular and extracellular polysaccharides of *Rhizobium japonicum* that bind soybean lectin. *J. Biol. Chem.* **1982**, *257*, 1870–1875.

(18) Pacchiano, R. A.; Sohn, W.; Chlanda, V. L.; Garbow, J. R.; Stark, R. E. Isolation and spectral characterization of plant cuticle polyesters. *J. Agric. Food Chem.* **1993**, *41*, 78–83.

(19) Mort, A. J. An apparatus for safe and convenient handling of anhydrous, liquid hydrogen fluoride at controlled temperatures and reaction times. Application to the generation of oligosaccharides from polysaccharides. *Carbohydr. Res.* **1983**, *122*, 315–321.

(20) Griesinger, C.; Otting, G.; Wuthrich, K.; Ernst, R. R. Clean TOCSY for ^{1}H spin system identification in macromolecules. *J. Am. Chem. Soc.* **1988**, *110*, 7870–7872.

(21) Muller, L. Sensitivity enhanced detection of weak nuclei using heteronuclear multiple quantum coherence. *J. Am. Chem. Soc.* **1979**, *101*, 4481–4484.

(22) Hwang, T.-L.; Shaka, A. J. Water Suppression that works. Excitation sculpting using arbitrary waveforms and pulsed field gradients. *J. Magn. Reson. A* **1995**, *112*, 275–279.

(23) Hurd, R. E.; John, B. K. Gradient enhanced proton-detected heteronuclear multiple-quantum coherence spectroscopy. *J. Magn. Reson.* **1991**, *91*, 648–653.

(24) Rinaldi, P. L.; Keifer, P. A. The utility of pulsed-field-gradient HMBC for organic structure determination. *J. Magn. Reson. A* **1994**, *108*, 259–262.

(25) Bax, A.; Summers, M. F. ^{1}H and ^{13}C assignments from sensitivity-enhanced detection of heteronuclear multiple-bond connectivity by 2D multiple quantum NMR. *J. Am. Chem. Soc.* **1986**, *108*, 2093–2094.

(26) Graca, J.; Schreiber, L.; Rodrigues, J.; Pereira, H. Glycerol and glyceryl esters of ω-hydroxyacids in cutins. *Phytochemistry* **2002**, *61*, 205–215.

(27) Bonaventure, G.; Beisson, F.; Ohlrogge, J.; Pollard, M. Analysis of the aliphatic monomer composition of polyesters associated with *Arabidopsis* epidermis: Occurrence of octadeca-cis-6,cis-9-diene-1,18-dioate as the major component. *Plant J.* **2004**, 920–930.

(28) Blee, E. Phytooxylipins and plant defense reactions. *Prog. Lipid Res.* **1998**, *37*, 33–72.

(29) Wasternack, C. Jasmonates: An update on biosynthesis, signal transduction and action in plant stress response, growth and development. *Ann. Bot.* **2007**, *100*, 681–697.

(30) Gerard, H. C.; Osman, S. F.; Fett, W. F.; Moreau, R. Separation, identification, and quantification of monomers from cutin polymers by high-performance liquid chromatography and evaporative light-scattering detection. *Phytochem. Anal.* **1992**, *3*, 139–144.

(31) Tian, S. Molecular structures of natural polymers: Cutin, suberin, and melanin. Ph.D. Thesis, 2005.

Received for review April 1, 2008. Revised manuscript received August 28, 2008. Accepted August 31, 2008. This work was supported by a grant from the National Science Foundation (MCB-0134705). The CUNY HPLC/MS facility (Agilent G1946D and 6210) is operated by Hunter College with support from NIH Shared Instrumentation Grant #1S10RR022649-01.

JF801028G